Dynamic partitioning of mitotic kinesin-5 cross-linkers between microtubule-bound and freely diffusing states

Dhanya K. Cheerambathur, Ingrid Brust-Mascher, Gul Civelekoglu-Scholey, and Jonathan M. Scholey

Department of Molecular and Cell Biology, University of California at Davis, Davis, CA 95616

The dynamic behavior of homotetrameric kinesin-5 during mitosis is poorly understood. Kinesin-5 may function only by binding, cross-linking, and sliding adjacent spindle microtubules (MTs), or, alternatively, it may bind to a stable "spindle matrix" to generate mitotic movements. We created transgenic *Drosophila melanogaster* expressing fluorescent kinesin-5, KLP61F-GFP, in a *klp61f* mutant background, where it rescues mitosis and viability. KLP61F-GFP localizes to interpolar MT bundles, half spindles, and asters, and is enriched around spindle poles. In fluorescence recovery after photobleaching experiments, KLP61F-GFP displays dynamic mobility similar to tubulin, which is inconsistent with a substantial static pool of kinesin-5. The data conform to a reaction–diffusion model in which most KLP61F is bound to spindle MTs, with the remainder diffusing freely. KLP61F appears to transiently bind MTs, moving short distances along them before detaching. Thus, kinesin-5 motors can function by cross-linking and sliding adjacent spindle MTs without the need for a static spindle matrix.

Introduction

Mitosis is mediated by the mitotic spindle (Walczak and Heald, 2008), whose assembly and function depends upon kinesin-5 motors (Valentine et al., 2006a). Purified kinesin-5 is a slow, plus end–directed bipolar homotetramer, capable of cross-linking and sliding adjacent microtubules (MTs; Sawin et al., 1992; Cole et al., 1994; Kashina et al., 1996; Kapitein et al., 2005; Tao et al., 2006). It moves in a modestly processive fashion, taking runs of ~10 steps along MT tracks before detaching (Valentine et al., 2006b; Krzysiak et al., 2008). Within cells, the mitotic functions of kinesin-5 depend upon its homotetrameric state (Hildebrandt et al., 2006). Thus kinesin-5 motors may serve as dynamic MT–MT cross-links that bundle parallel MTs and drive an antiparallel MT-based sliding filament mechanism (McIntosh et al., 1969) to contribute to mitotic spindle morphogenesis and function (Saunders and Hoyt, 1992; Heck et al., 1993; Walczak et al., 1998; Sharp et al., 2000; Goshima and Vale, 2003; Brust-Mascher et al., 2004; Miyamoto et al., 2004; Civelekoglu-Scholey and Scholey, 2007; Saunders et al., 2007).

Although it is plausible that kinesin-5 need interact only with MTs to perform its mitotic functions (e.g., Brust-Mascher et al., 2004), an alternative hypothesis proposes that kinesin-5 may interact with a hypothetical non-MT "spindle matrix," which could serve as a supporting structure against which mitotic motors exert force on MTs to generate mitotic movements (Kapoor and Mitchison, 2001; Chang et al., 2004; Tsai et al., 2006; Johansen and Johansen, 2007). These two mechanisms might give rise to different types of dynamic behavior by kinesin-5 if, for example, the highly dynamic spindle MTs, which turn over rapidly by dynamic instability and poleward flux, display different dynamic properties from a relatively stable matrix. Thus, an evaluation of the dynamic properties of kinesin-5 within different spindles is warranted (discussed in Kapoor and Mitchison, 2001). Here, we compared the dynamic properties of kinesin-5 and MTs in *Drosophila melanogaster* embryo mitotic spindles (Brust-Mascher and Scholey, 2007) through the analysis of transgenic flies expressing functional KLP61F-GFP.

Results and discussion

Transgenic flies expressing functional KLP61F-GFP

To study the dynamics of KLP61F in vivo, standard fly genetics and transformation techniques (Roberts, 1986; Ashburner, 1989)

Correspondence to Jonathan M. Scholey: jmscholey@ucdavis.edu

Abbreviations used in this paper: FSM, fluorescence speckle microscopy; ipMT, interpolar MT; kMT, kinetochore MT; MT, microtubule.

The online version of this paper contains supplemental material.

The Rockefeller University Press $30.00
J. Cell Biol. Vol. 182 No. 3 429–436
www.jcb.org/cgi/doi/10.1083/jcb.200804100

were used to generate stable transgenic fly lines expressing KLP61F-GFP under the control of a poly-ubiquitin promoter in a form that localizes to spindles and supports mitosis (Fig. 1). This promoter drives near normal levels of KLP61F because quantitative immunoblotting revealed that wild-type embryos harboring two copies of the transgene contained KLP61F-GFP/endogenous KLP61F in the ratio 0.4–0.7:1.0. Also, KLP61F-GFP displayed similar spindle localization and dynamics in either the presence (unpublished data) or absence (see below) of wild-type KLP61F, which suggests that it can compete effectively with endogenous untagged KLP61F for binding sites in spindles. One or two copies of the KLP61F-GFP transgene were able to rescue several null or severe loss-of-function mutant alleles (namely *klp61f*^{3}, *klp61f*^{4}, *klp61f*^{6836}, and *klp61f*^{7415}) that, in the absence of the rescuing transgene, only survive as homozygotes or transheterozygotes to second or third instar larval stages, when they die due to mitotic failures when the maternal load of KLP61F is depleted (Heck et al., 1993). For example, *klp61f*^{3}/*klp61f*^{3} homozygotes and *klp61f*^{3}/*klp61f*^{6836} transheterozygotes display larval lethality but were rescued by either one or two copies of the KLP61F-GFP transgene and produced viable, fertile adult flies that could be propagated as stable transgenic lines, which suggests that the KLP61F-GFP is functional (studies described in the following sections refer to the latter mutant rescued with two copies of the transgene). As with transgenic lines expressing other fluorescent mitotic proteins (e.g., GFP-Ncd; Endow and Komma, 1997), these KLP61F-GFP–expressing lines should be useful for studying mitosis in various *D. melanogaster* cell types.

The functionality of GFP-KLP61F was further assessed by careful analysis of the dynamics of spindle pole separation (Fig. 1 B). Plots of pole–pole separation versus time for the rescued mutant were similar to those of wild-type embryos (for comparison, anti-KLP61F–induced prometaphase spindle collapse is presented instead of unrescued mutants, whose lethality makes corresponding plots impossible; Sharp et al., 2000). KLP61F-GFP embryos displayed a decrease in the rate of prometaphase-to-metaphase spindle elongation (0.017 μm/s) compared with wild-type embryos (0.03 μm/s), which led to a small decrease in subsequent spindle length, but otherwise, the plots are identical. Thus, KLP61F-GFP is almost fully functional.

Localization of kinesin-5 in mitotic spindles

Previous immunofluorescence and immuno-EM with anti–phospho-KLP61F antibody showed that, within *D. melanogaster* embryos, bipolar KLP61F motors (Cole et al., 1994; Kashina et al., 1996) localize to interphase nuclei and throughout mitotic spindles, forming presumptive cross-bridges between adjacent MTs (Sharp et al., 1999). Here, we examined living rather than fixed embryos by spinning disc confocal microscopy and observed that KLP61F-GFP displayed a fibrous colchicine-sensitive colocalization with fluorescent tubulin (Fig. 1 A and Video 1, available at http://www.jcb.org/cgi/content/full/jcb.200804100/DC1; see Fig. 4 C). During interphase/prophase, KLP61F-GFP localizes to centrosomes and astral MTs. After nuclear envelope breakdown, KLP61F associates with MTs spanning the equator, and by metaphase, it localizes along all observable MT bundles, which indicates an association with both kinetochore MT (kMT) and interpolar MT (ipMT) fibers, being somewhat concentrated around the spindle pole. Significantly, throughout anaphase B, when chromosomes have moved to the poles so that the kMTs have disassembled (Brust-Mascher and Scholey, 2002), KLP61F-GFP clearly localizes on the ipMTs spanning the pole–pole axis (Sharp et al., 1999). During early anaphase B, KLP61F-GFP localizes uniformly along ipMT bundles, but during late anaphase B, it appears more concentrated at the spindle equator. Finally, it localized to the telophase midbody, except at a small ∼0.6-μm-wide central region.

Generally, this localization is consistent with proposals that KLP61F acts on dynamic ipMTs to exert outward forces on spindle poles, which maintains the prometaphase spindle against antagonistic inward forces and drives anaphase B spindle elongation (Heck et al., 1993; Sharp et al., 2000; Brust-Mascher and Scholey, 2002; Brust-Mascher et al., 2004; Tao et al., 2006). However, two observations differ from those made previously (Sharp et al., 1999). First, KLP61F-GFP was present on interphase/prophase asters, with none being detected inside the nucleus, and second, we observed relatively high concentrations of the motor around metaphase spindle poles. The astral localization is consistent with previous observations in *D. melanogaster* S2 cells (Goshima and Vale, 2005) and embryos (Silverman-Gavrila and Wilde, 2006) and suggests that KLP61F may contribute to early spindle pole separation, although inhibiting KLP61F does not block the initial assembly of bipolar prometaphase spindles but instead induces their subsequent collapse (Fig. 1 B; Sharp et al., 2000). In addition, students of kinesin-5 in *Xenopus laevis* egg extracts have drawn attention to the high concentration of Eg5 around spindles poles (Sawin et al., 1992; Kapoor and Mitchison, 2001), and our results suggest that this may be conserved in *D. melanogaster* embryos.

Kinesin-5 is highly dynamic within mitotic spindles

KLP61F-GFP is extremely dynamic within spindles of living embryos and displays a striking redistribution at anaphase onset. For example, kymographs reveal that KLP61F and tubulin form a concentration gradient in the spindle based on fluorescence intensity, which is highest around the spindle poles and lowest at the equator (Fig. 2 A). At the onset of anaphase B, this gradient diminishes so that a more uniform distribution of both proteins is observed along the pole–pole axis; this is caused by net depletion of KLP61F (together with tubulin) from around the poles, based on scans of total KLP61F fluorescence intensity at the poles, the equator, and throughout the entire spindle (Fig. 2 B). This plausibly reflects KLP61F's dissociation from kMTs and short ipMTs that depolymerize around the poles (Brust-Mascher and Scholey, 2002; Cheerambathur et al., 2007) or its cell cycle–dependent proteolysis (Gordon and Roof, 2001). In contrast, the total intensity of KLP61F-GFP remains relatively constant at the spindle equator (Fig. 2 B), although line scans of fluorescence intensity drawn specifically along ipMT bundles (Fig. 1 A, right) reveal a slight increase in its intensity relative to tubulin at the equator at anaphase B onset.

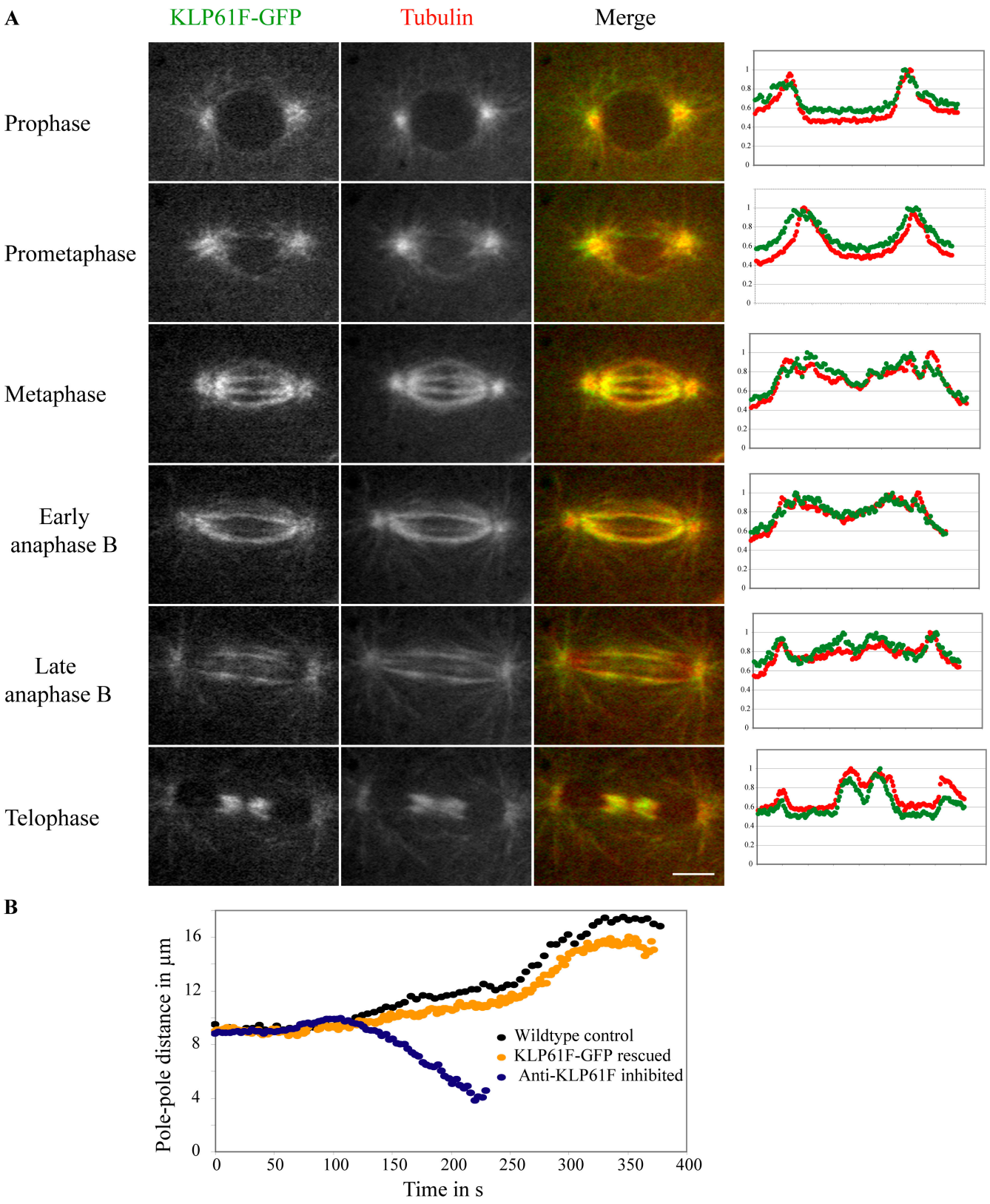

Figure 1. **Localization and function of KLP61F-GFP in *D. melanogaster* embryo mitosis.** (A) Micrographs from a time-lapse video of a representative spindle showing KLP61F-GFP (left), rhodamine-tubulin (center), and double-label fluorescence (right) at various stages of mitosis. The plots (far right) are line scans extending pole to pole along an ipMT (10 pixels wide; ~0.129 µm/pixel) for KLP61F (green) and tubulin (red). The y axis shows normalized fluorescence intensity. Bar, 5 µm. (B) Spindle pole dynamics in wild-type embryos, GFP-KLP61F rescued mutant embryos, and anti-KLP61F microinjected wild-type embryos showing how bipolar spindles collapse into monoasters after the loss of KLP61F function. Pole–pole separation dynamics are very similar in wild-type and rescued mutant embryos.

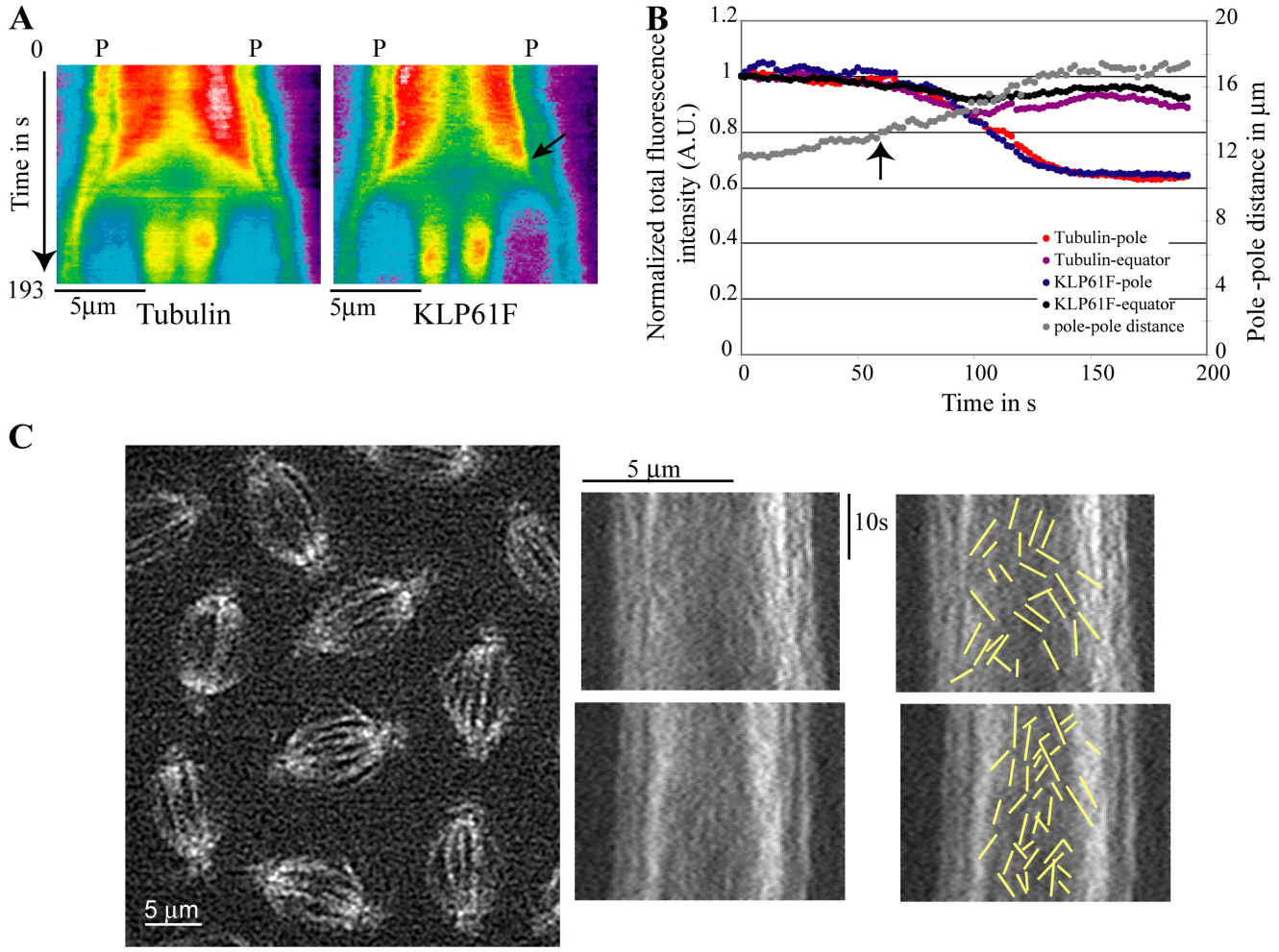

Figure 2. **Kymography and FSM of KLP61F-GFP dynamics.** (A) Kymographs of tubulin and KLP61F distribution from mid-metaphase (0 s) until telophase. In anaphase B, KLP61F moves toward the spindle equator before tubulin. Kymographs show the mean total intensity per pixel along the pole (P)–pole axis. Red and dark blue indicate the highest and lowest intensity, respectively. (B) Plot of normalized integrated fluorescence intensity of KLP61F and tubulin within a 2-µm-wide region along the pole–pole axis of the same spindle near the pole and equator during the preanaphase B–to–anaphase B transition (0 s = late metaphase). Arrows in A and B indicate anaphase B onset, i.e., when chromatids have separated and the spindle elongates at a characteristic linear rate (from 13 to 17 µm). (C, left) A frame from an FSM video showing KLP61F-GFP speckles on spindles. Kymographs from same video (center) display many speckles as "dots" rather than lines, which indicates transient binding of KLP61F to spindle MTs. (right) Tracings (overlaid on kymograph) showing a subset of speckles that appear as lines due to KLP61F motility (see text).

This increase in equatorial KLP61F may act in concert with ipMT reorganization to facilitate force generation for anaphase B (Sharp et al., 2000; Brust-Mascher et al., 2004; Cheerambathur et al., 2007).

KLP61F appears to take short "runs"

By fluorescence speckle microscopy (FSM) and kymography (Fig. 2 C), KLP61F-GFP speckles appear as "dots" or very short lines, much shorter than those formed by fluorescent tubulin in this system. These could correspond to functional fluorescent kinesin-5 particles that transiently bind and cross-link adjacent MTs, then move along them for short distances before detaching (Valentine et al., 2006b; Krzysiak et al., 2008). Such dynamic cross-linkers could bundle adjacent parallel MTs and slide apart antiparallel MTs, but given the relevant rates of KLP61F-driven motility (Cole et al., 1994; Tao et al., 2006) and MT flux and sliding (Brust-Mascher and Scholey, 2002), the motion of KLP61F-GFP speckles would be balanced by poleward flux or ipMT sliding so that the speckles would appear stationary. Higher resolution optics would be needed to routinely detect such activity, but of 460 speckle lines tracked in 10 spindles, 54 were vertical, and their mean length along the time axis was 2.1 ± 1.2 s (e.g., a few such lines are visible in Fig. 2 C). These may correspond to stationary KLP61F-GFP particles that cross-link adjacent MTs and run along them typically for the order of 100 nm (i.e., 2.1 s at 0.04 µm/s = 84 nm or 10 steps; Cole et al., 1994; Valentine et al., 2006b). This interpretation is consistent with previous immuno-EM, in which we observed KLP61F molecules cross-bridging adjacent MTs throughout embryonic spindles (Sharp et al., 1999). Our observations differ from those made on Eg5 in *X. laevis* extract spindles, where far more abundant, robust, and persistent stationary tracks were seen and were interpreted as being Eg5 molecules bound to a stationary spindle matrix (Kapoor and Mitchison, 2001). The remaining 406 tracked speckles produced diagonal lines moving 10-fold faster than KLP61F, 0.34 ± 0.24 µm/s

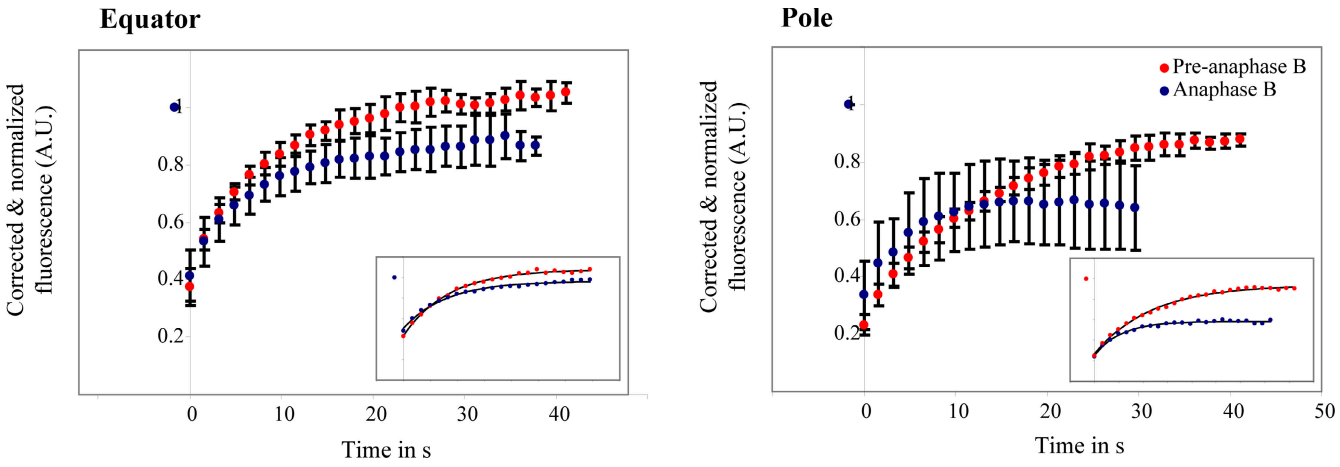

Figure 3. **FRAP analysis of KLP61F-GFP in *D. melanogaster* embryo spindles.** KLP61F turns over rapidly. Plots show corrected (see Materials and methods) normalized fluorescence recovery of a 2-µm-wide region at the equator and pole during preanaphase B and anaphase B. (insets) Representative plots for individual experiments. Each curve was fitted with a single exponential (black line). Error bars represent standard deviation (see Table I).

(Fig. 2 C), which could be KLP61F-GFP molecules being transported poleward or antipoleward to specific sites within the spindle, e.g., by another mitotic motor (Kapoor and Mitchison, 2001) or by surfing on the ends of dynamic MTs (Cheerambathur et al., 2007).

Kinesin-5 and spindle MTs behave as a reaction–diffusion system

FRAP analysis of KLP61F-GFP dynamics within mitotic spindles, in combination with quantitative modeling, suggests that KLP61F conforms to a "reaction–diffusion" system, and partitions only between MT-bound and freely diffusing states (Fig. 3 and Tables I and II; Brust-Mascher et al., 2004; Cheerambathur et al., 2007). After correcting for photobleaching (see Materials and methods), it became clear that KLP61F-GFP turns over completely and rapidly with a half-time of 3–9 s throughout preanaphase B and anaphase B. This is remarkably similar to the dynamics of tubulin in these spindles (Cheerambathur et al., 2007), which is consistent with our visual impression that KLP61F colocalizes with spindle MTs (Fig. 1). After photobleaching, the extent of fluorescence recovery was near complete at all regions except the poles during anaphase B (see the following paragraph), which is consistent with KLP61F being bound to spindle MTs, with no evidence for binding to any more stable structure in the spindle, such as a stable "skeletor-like" matrix (Kapoor and Mitchison, 2001; Johansen and Johansen, 2007). This interpretation is supported by our observation that KLP61F localization to the spindle depends upon intact MTs and is disrupted by colchicine-induced MT disassembly (Fig. 4 C).

The one exception to the observed total recovery of fluorescence from photobleaching was at the poles during anaphase B (Table I). Careful examination reveals that this is mainly caused by the loss of KLP61F-GFP from around the pole, which is consistent with the 30–40% loss in mean fluorescence observed in an identical-sized region of an unbleached spindle pole (even after correction for low levels of background photobleaching) and as also observed by kymography as noted previously (Fig. 2, A and B). It is plausible that this loss is related to the previously described establishment of an MT "catastrophe gradient" at anaphase B onset in this system, which leads to the depolymerization of short MTs near the poles, whereas longer ipMTs grow by polymerization at their plus ends to invade the spindle equator (Cheerambathur et al., 2007). The depolymerization of these short ipMTs and that of kMTs during late phases of chromatid-to-pole motility, as well as the associated loss of KLP61F bound to these depolymerizing MTs, and its translocation along stable ipMTs to the equator (Fig. 1 A), could easily account for the loss of KLP61F-GFP fluorescence around the poles, and may also contribute to the higher variance in the FRAP recovery curves in this region (Fig. 3). Also, although tubulin and KLP61F fluorescence decreases near the poles during anaphase B by 30–40% (Figs. 1 A and 2, A and B), after photobleaching, tubulin and KLP61F display up to 45% (Cheerambathur et al., 2007) and 51% recovery on average. Taken together, the results are consistent with the idea that, during anaphase B, the KLP61F motors that bind to the stable pole-associated minus end regions of the long ipMTs, whose plus ends invade the equator (Cheerambathur et al., 2007),

Table I. **KLP61F turnover during metaphase and anaphase B in spindles of *D. melanogaster* embryos**

	Near pole		Equator	
	$t_{1/2}$ in s	% recovery	$t_{1/2}$ in s	% recovery
Preanaphase B	8.8 ± 0.6 (n = 4)	87 ± 4 (n = 4)	5.9 ± 0.3 (n = 5)	108 ± 7 (n = 5)
Anaphase B	3.0 ± 0.6 (n = 5)	51 ± 16[a] (n = 5)	5.4 ± 0.2 (n = 4)	79 ± 10 (n = 4)

[a]Note that this apparent decrease in recovery around the poles is due to the net loss of both tubulin and KLP61F in this region rather than being due to a stable population of KLP61F that turns over slowly (see text).

Table II. **Fraction of MT-bound and freely diffusing KLP61F motors**

	Near pole		Equator	
	% bound motors	% free motors	% bound motors	% free motors
Preanaphase B	90 ± 1 (n = 4)	10 ± 1 (n = 4)	85 ± 2 (n = 5)	15 ± 2 (n = 5)
Anaphase B	71 ± 6 (n = 5)	29 ± 6 (n = 5)	86 ± 0 (n = 4)	14 ± 0 (n = 4)

continue to turnover rapidly. Thus, these motors appear to display rapid, transient binding to and dissociation from stable (as well as dynamic) MT tracks, which is consistent with the in vitro behavior of kinesin-5 (Valentine et al., 2006b; Krzysiak et al., 2008).

By modeling KLP61F-GFP dynamics as a simple reaction–diffusion system characterized by binding and dissociation of kinesin-5 to and from MTs interspersed with free diffusion, we estimate that KLP61F is substantially (generally >85%) bound to spindle MTs, with a small fraction (10–15%) being freely diffusible, and this analysis provides no evidence for a stable subpopulation being bound to a spindle matrix (Tables I and II; See Materials and methods). Also, the unique behavior of KLP61F around the pole (only 71% bound and 29% freely diffusing) supports the idea that the loss of KLP61F from the poles is caused by enhanced dissociation of the motor from (stable or depolymerizing) MTs rather than being caused by proteolysis. Clearly, the dynamics and functions of KLP61F and MTs around spindle poles merit further analysis.

Kinesin-5 function requires Thr-933

The phosphorylatable Thr-933 residue in the bimC box of kinesin-5 is thought to target kinesin-5 to spindles in *X. laevis* and *D. melanogaster* (Sawin and Mitchison, 1995; Sharp et al., 1999). Consistent with this, when KLP61F-GFP containing either Thr-933–to–Ala or Thr-933–to–Aspartate mutations was expressed in wild-type embryos, it displayed only a very weak, nonfibrous localization to spindles, which is very similar to the results of Sawin and Mitchison (1995; Fig. 4). The low level in the spindle may represent the formation of mutant KLP61F-GFP/wild-type KLP61F hetero-oligomers, which bind weakly to MTs; the abnormal, weak binding of the mutants to a non-MT spindle structure; or the abnormal sequestration of the mutants within the spindle envelope (Sharp et al., 1999). Significantly, unlike

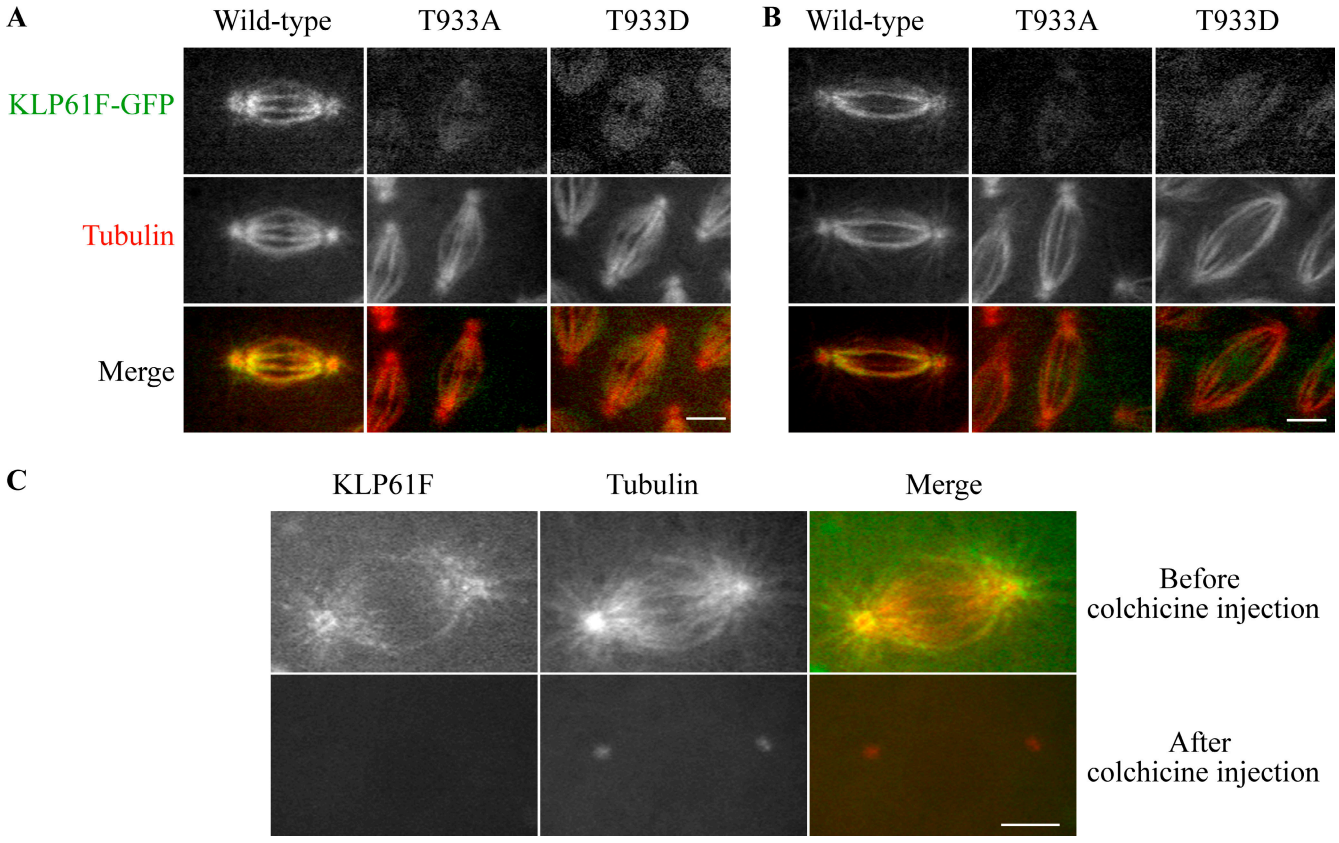

Figure 4. **Localization of wild-type and bimC-box mutant KLP61F.** Distribution of KLP61FT933A-GFP and KLP61FT933D-GFP point mutants compared with wild-type KLP61F-GFP during metaphase (A) and anaphase B (B) in embryos injected with rhodamine-tubulin to mark MTs. The mutants barely associate with spindle MTs. (C) Localization of wild-type KLP61F-GFP to spindles is MT dependent. (top) Prometaphase KLP61F-GFP embryos containing rhodamine tubulin were imaged, transferred to a microinjection microscope, and injected with 25 mg/ml colchicine. (bottom) 3D projections 3 min later, after transfer back to the spinning disc microscope, show that spindle MTs were depolymerized, which results in a complete loss of KLP61F-GFP. Bars, 5 µm.

nonmutant KLP61F-GFP, neither Thr-933 mutant was capable of rescuing the *klp61f* mutants, which suggests that Thr-933 has an essential role and provides a suitable control for the functionality of the wild-type protein.

Relation of our study to previous studies of kinesin-5 dynamics

In *X. laevis* extracts, fluorescent antibody labeling revealed Eg5 speckles moving toward the plus ends of astral MTs at ~3 µm/min, although it is unclear if the antibody perturbed the motor's dynamics (Wilde et al., 2001). In such extracts, chemically modified, functional fluorescent Eg5 speckles remained stationary on MT tracks undergoing poleward flux in the presence or absence of the Eg5 inhibitor monastrol, leading to proposals that kinesin-5 motors are normally immobilized and slide MTs against a stable spindle matrix, as in in vitro MT "gliding assays" (Kapoor and Mitchison, 2001). The spindle localization of the kinesin-5 KLP61F-GFP in *D. melanogaster* S2 cells is colchicine sensitive, and thus depends upon intact MTs, as we have now confirmed in embryos (Fig. 4 C), although the dynamics of the motor were not examined (Goshima and Vale, 2005). Our studies are the first to show that fluorescent kinesin-5, which, based on mutant rescue can support normal mitosis (Fig. 1 B), displays dynamic properties consistent with its association only with MTs and not with another stable structure in spindles.

Implications for mitosis

Our data suggest that KLP61F partitions between freely diffusing and MT-bound states. During transient binding to MTs throughout the spindle, KLP61F may take short runs, typically of the order of <100 nm, along adjacent MTs before detaching, which is consistent with in vitro data (Valentine et al., 2006b; Krzysiak et al., 2008) and consistent with the idea that the motor cross-links parallel MTs into bundles but cross-links and slides apart antiparallel MTs (McIntosh et al., 1969; Sharp et al., 1999). Our data provide no evidence for substantial binding of kinesin-5 to a stationary spindle matrix in *D. melanogaster* embryos, but we are cautious about generalizing our conclusions because we cannot eliminate the possibility that other motors bind such a matrix in *D. melanogaster* embryos, or that a spindle matrix, possibly working in concert with kinesin-5, plays important roles elsewhere (Kapoor and Mitchison, 2001; Chang et al., 2004; Tsai et al., 2006; Johansen and Johansen, 2007). Our data also do not eliminate the binding of kinesin-5 to a matrix with similar dynamics to tubulin, though it is unclear what functional advantage this would provide. KLP61F-GFP is depleted from spindle poles at anaphase onset, but it does remain localized along ipMTs throughout anaphase B. Because ipMT plus ends "invade" the central spindle at anaphase B onset (Cheerambathur et al., 2007), this predicts a corresponding increase in the number of antiparallel ipMTs having KLP61F bound at the spindle equator. Modeling suggests that, at the equator, multiple bipolar KLP61F motors could cross-link and slide apart highly dynamic, growing and shrinking antiparallel MT tracks, and in the absence of any additional mechanical substrate, generate forces to drive the steady, linear rate of spindle elongation characteristic of anaphase B (Brust-Mascher et al., 2004). Dynamic cross-linkers whose dynamic properties match those of tubulin, like those inferred here, would be well-adapted for carrying out this function.

Materials and methods

Generation of transgenic flies

A full-length KLP61F cDNA tagged to GFP in a pMT vector, provided by G. Goshima (Nagoya University, Nagoya, Aichi, Japan) and R. Vale (University of California, San Francisco, San Francisco, CA) was subcloned into the pWR-pUbq transformation vector (provided by N. Brown, University of Cambridge, Cambridge, England, UK) downstream of the polyubiquitin promoter. The point mutants KLP61FT933A-GFP and KLP61FT933D-GFP were generated by site-directed mutagenesis of the above construct using a mutagenesis kit (Stratagene). The above constructs were injected into w− flies to generate transgenic flies at Bestgene Inc. Flies with a single insertion into either the X, second, or third chromosome were obtained. Rescue crosses were done by crossing the transgenic lines into *klp61f* mutants (provided by M. Heck, University of Edinburgh, Edinburgh, Scotland, UK; A. Pereira, University of Massachusetts, Worcester, MA; and P. Wilson, Georgia State University, Atlanta, GA) by standard genetic methods.

D. melanogaster stocks and embryo preparation

Flies were maintained at 25°C, and 0–2-h-old embryos were collected as described previously (Ashburner, 1989).

Microscopy and image analysis

FRAP experiments were done on a laser-scanning confocal microscope (FV1000) with a 60× 1.40 NA objective at 23°C (both from Olympus), and image acquisition was done using the Fluoview software (version 1.5; Olympus). The embryos expressing KLP61F-GFP were dechorionated and kept in halocarbon oil to prevent dehydration and were imaged using the 488-nm line from an argon laser. A separate 405-nm laser was used to photobleach KLP61F-GFP. The spindle was bleached in rectangular areas of defined dimensions, and images were acquired every 1.6 s. Time-lapse microscopy of KLP61F-GFP–expressing embryos was done on a microscope (Olympus) equipped with an UltraView spinning disk confocal head (PerkinElmer) with a 100× 1.35 NA objective (Olympus). Images were acquired using UltraView software (PerkinElmer) at a rate of 1. 9 s per frame at 23°C, and recorded using a digital camera (ORCA ER; Hamamatsu). Embryos were injected with rhodamine tubulin (Cytoskeleton, Inc.) to visualize MTs. Images were analyzed using MetaMorph (MDS Analytical Technologies). The images were processed using the "No Neighbors" deconvolution and low pass filter commands. For kymographs of KLP61F-GFP speckles, images were taken at a rate of 3 frames per second. A background image obtained outside the focal plane was subtracted and the No Neighbors deconvolution or the Sharpen High command was applied followed by a low pass filter. Kymographs were obtained from ipMT bundles. For 3D reconstruction in Fig. 4 C, the z stacks were acquired at 0.5-µm steps, and the projections were generated in MetaMorph.

FRAP data analysis

The spindles were corrected for movement using MatLab (The Mathworks, Inc.), and the fluorescence intensities within the bleached region were measured using MetaMorph imaging software. All data were corrected for photobleaching and normalized by $I(t) = [F(t)T_{pre}]/[T(t)F_{pre}]$, where F(t) and T(t) are the mean fluorescence in the FRAP region and in the entire spindle at time t, and F_{pre} and T_{pre} are the mean fluorescence in the FRAP region and in the entire spindle just before the bleach (Phair and Misteli, 2000; Lele et al., 2006). The percent recovery was obtained by calculating the fraction $(F_{inf}-F_0)/(F_{pre}-F_0)$, where F_0 is the mean intensity in the FRAP region just after bleaching and F_{inf} is the final fluorescence obtained from the fit (Bulinski et al., 2001). The data were modeled as a reaction–diffusion process in which motors bind to and dissociate from MTs and then undergo free diffusion in the spindle. Based on the lack of a biphasic appearance of the experimental recovery curve after correction for photobleaching, we considered a suitable model to be one in which the exact solution to the reaction–diffusion process, incorporating boundary and initial conditions, could be well approximated by slow diffusion in the form of a single exponential. Accordingly, an effective diffusion model in a rectangular bleach region was used to fit the data (Carrero et al., 2004). The fit to the data yielded several parameters, including the initial and final normalized fluorescence intensities and the recovery half-time. In addition, the derived effective diffusion process time constant (~5), together with the fraction of

fluorescence loss in the entire spindle just after photobleaching (5–30%) and the estimate of the diffusion coefficient of KLP61F ~1 $\mu m^2/s$ (based on data collected in a region that was bleached outside the spindle, where motors are presumably diffusing freely, and through a simple calculation [$D \sim M^{-1/3}$]), yielded estimates of the fraction of bound to free motors in the FRAP region (with a free diffusion transfer coefficient of ~0.5; Carrero et al., 2004). The model was fit to experimental data using Excel (Microsoft) and the Easyfit function of MatLab with a user-defined function or the routine *nlinfit*. All R^2 values are above 0.95, and residuals are randomly distributed around zero.

Online supplemental material

Video 1 shows KLP61F-GFP dynamics during mitosis in *D. melanogaster* syncytial embryonic spindles. See Fig. 1. Online supplemental material is available at http://www.jcb.org/cgi/content/full/jcb.200804100/DC1.

We thank Drs. Gohta Goshima and Ron Vale for generously supplying the KLP61F-GFP–expressing plasmid, and Drs. Margarete Heck, Andrea Pereira, and Patricia Wilson for providing klp61f mutant stocks.

This work was supported by National Institutes of Health (NIH) grant GM55507 to J.M. Scholey. G. Civelekoglu-Scholey was partially supported by NIH grant GM068952 to J.M. Scholey and A. Mogilner, and NIH grant GM068952 to A. Mogilner.

Submitted: 17 April 2008
Accepted: 7 July 2008

References

Ashburner, M. 1989. Drosophila: A Laboratory Handbook. Cold Spring Harbor Laboratory Press, Cold Spring Harbor, NY. 1,331 pp.

Brust-Mascher, I., and J.M. Scholey. 2002. Microtubule flux and sliding in mitotic spindles of *Drosophila* embryos. *Mol. Biol. Cell.* 13:3967–3975.

Brust-Mascher, I., and J.M. Scholey. 2007. Mitotic spindle dynamics in *Drosophila*. *Int. Rev. Cytol.* 259:139–172.

Brust-Mascher, I., G. Civelekoglu-Scholey, M. Kwon, A. Mogilner, and J.M. Scholey. 2004. Model for anaphase B: role of three mitotic motors in a switch from poleward flux to spindle elongation. *Proc. Natl. Acad. Sci. USA.* 101:15938–15943.

Bulinski, J.C., D.J. Odde, B.J. Howell, T.D. Salmon, and C.M. Waterman-Storer. 2001. Rapid dynamics of the microtubule binding of ensconsin in vivo. *J. Cell Sci.* 114:3885–3897.

Carrero, G., E. Crawford, M.J. Hendzel, and G. de Vries. 2004. Characterizing fluorescence recovery curves for nuclear proteins undergoing binding events. *Bull. Math. Biol.* 66:1515–1545.

Chang, P., M.K. Jacobson, and T.J. Mitchison. 2004. Poly(ADP-ribose) is required for spindle assembly and structure. *Nature.* 432:645–649.

Cheerambathur, D.K., G. Civelekoglu-Scholey, I. Brust-Mascher, P. Sommi, A. Mogilner, and J.M. Scholey. 2007. Quantitative analysis of an anaphase B switch: predicted role for a microtubule catastrophe gradient. *J. Cell Biol.* 177:995–1004.

Civelekoglu-Scholey, G., and J.M. Scholey. 2007. Mitotic motors: kinesin-5 takes a brake. *Curr. Biol.* 17:R544–R547.

Cole, D.G., W.M. Saxton, K.B. Sheehan, and J.M. Scholey. 1994. A "slow" homotetrameric kinesin-related motor protein purified from *Drosophila* embryos. *J. Biol. Chem.* 269:22913–22916.

Endow, S.A., and D.J. Komma. 1997. Spindle dynamics during meiosis in *Drosophila* oocytes. *J. Cell Biol.* 137:1321–1336.

Gordon, D.M., and D.M. Roof. 2001. Degradation of the kinesin Kip1p at anaphase onset is mediated by the anaphase-promoting complex and Cdc20p. *Proc. Natl. Acad. Sci. USA.* 98:12515–12520.

Goshima, G., and R.D. Vale. 2003. The roles of microtubule-based motor proteins in mitosis: comprehensive RNAi analysis in the *Drosophila* S2 cell line. *J. Cell Biol.* 162:1003–1016.

Goshima, G., and R.D. Vale. 2005. Cell cycle-dependent dynamics and regulation of mitotic kinesins in *Drosophila* S2 cells. *Mol. Biol. Cell.* 16:3896–3907.

Heck, M.M., A. Pereira, P. Pesavento, Y. Yannoni, A.C. Spradling, and L.S. Goldstein. 1993. The kinesin-like protein KLP61F is essential for mitosis in *Drosophila*. *J. Cell Biol.* 123:665–679.

Hildebrandt, E.R., L. Gheber, T. Kingsbury, and M.A. Hoyt. 2006. Homotetrameric form of Cin8p, a *Saccharomyces cerevisiae* kinesin-5 motor, is essential for its in vivo function. *J. Biol. Chem.* 281:26004–26013.

Johansen, K.M., and J. Johansen. 2007. Cell and molecular biology of the spindle matrix. *Int. Rev. Cytol.* 263:155–206.

Kapitein, L.C., E.J. Peterman, B.H. Kwok, J.H. Kim, T.M. Kapoor, and C.F. Schmidt. 2005. The bipolar mitotic kinesin Eg5 moves on both microtubules that it crosslinks. *Nature.* 435:114–118.

Kapoor, T.M., and T.J. Mitchison. 2001. Eg5 is static in bipolar spindles relative to tubulin: evidence for a static spindle matrix. *J. Cell Biol.* 154:1125–1133.

Kashina, A.S., R.J. Baskin, D.G. Cole, K.P. Wedaman, W.M. Saxton, and J.M. Scholey. 1996. A bipolar kinesin. *Nature.* 379:270–272.

Krzysiak, T.C., M. Grabe, and S.P. Gilbert. 2008. Getting in sync with dimeric Eg5. Initiation and regulation of the processive run. *J. Biol. Chem.* 283:2078–2087.

Lele, T., S.R. Wagner, J.A. Nickerson, and D.E. Ingber. 2006. Methods for measuring rates of protein binding to insoluble scaffolds in living cells: histone H1-chromatin interactions. *J. Cell. Biochem.* 99:1334–1342.

McIntosh, J.R., P.K. Hepler, and D.G. Van Wie. 1969. Model for mitosis. *Nature.* 224:659–663.

Miyamoto, D.T., Z.E. Perlman, K.S. Burbank, A.C. Groen, and T.J. Mitchison. 2004. The kinesin Eg5 drives poleward microtubule flux in *Xenopus laevis* egg extract spindles. *J. Cell Biol.* 167:813–818.

Phair, R.D., and T. Misteli. 2000. High mobility of proteins in the mammalian cell nucleus. *Nature.* 404:604–609.

Roberts, D. 1986. *Drosophila*: A Practical Approach. IRL Press, Oxford. 296 pp.

Saunders, W.S., and M.A. Hoyt. 1992. Kinesin-related proteins required for structural integrity of the mitotic spindle. *Cell.* 70:451–458.

Saunders, A.M., J. Powers, S. Strome, and W.M. Saxton. 2007. Kinesin-5 acts as a brake in anaphase spindle elongation. *Curr. Biol.* 17:R453–R454.

Sawin, K.E., and T.J. Mitchison. 1995. Mutations in the kinesin-like protein Eg5 disrupting localization to the mitotic spindle. *Proc. Natl. Acad. Sci. USA.* 92:4289–4293.

Sawin, K.E., K. LeGuellec, M. Philippe, and T.J. Mitchison. 1992. Mitotic spindle organization by a plus-end-directed microtubule motor. *Nature.* 359:540–543.

Sharp, D.J., K.L. McDonald, H.M. Brown, H.J. Matthies, C. Walczak, R.D. Vale, T.J. Mitchison, and J.M. Scholey. 1999. The bipolar kinesin, KLP61F, cross-links microtubules within interpolar microtubule bundles of *Drosophila* embryonic mitotic spindles. *J. Cell Biol.* 144:125–138.

Sharp, D.J., H.M. Brown, M. Kwon, G.C. Rogers, G. Holland, and J.M. Scholey. 2000. Functional coordination of three mitotic motors in *Drosophila* embryos. *Mol. Biol. Cell.* 11:241–253.

Silverman-Gavrila, R.V., and A. Wilde. 2006. Ran is required before metaphase for spindle assembly and chromosome alignment and after metaphase for chromosome segregation and spindle midbody organization. *Mol. Biol. Cell.* 17:2069–2080.

Tao, L., A. Mogilner, G. Civelekoglu-Scholey, R. Wollman, J. Evans, H. Stahlberg, and J.M. Scholey. 2006. A homotetrameric kinesin-5, KLP61F, bundles microtubules and antagonizes Ncd in motility assays. *Curr. Biol.* 16:2293–2302.

Tsai, M.Y., S. Wang, J.M. Heidinger, D.K. Shumaker, S.A. Adam, R.D. Goldman, and Y. Zheng. 2006. A mitotic lamin B matrix induced by RanGTP required for spindle assembly. *Science.* 311:1887–1893.

Valentine, M.T., P.M. Fordyce, and S.M. Block. 2006a. Eg5 steps it up! *Cell Div.* 1:31.

Valentine, M.T., P.M. Fordyce, T.C. Krzysiak, S.P. Gilbert, and S.M. Block. 2006b. Individual dimers of the mitotic kinesin motor Eg5 step processively and support substantial loads in vitro. *Nat. Cell Biol.* 8:470–476.

Walczak, C.E., and R. Heald. 2008. Mechanisms of mitotic spindle assembly and function. *Int. Rev. Cytol.* 265:111–158.

Walczak, C.E., I. Vernos, T.J. Mitchison, E. Karsenti, and R. Heald. 1998. A model for the proposed roles of different microtubule-based motor proteins in establishing spindle bipolarity. *Curr. Biol.* 8:903–913.

Wilde, A., S.B. Lizarraga, L. Zhang, C. Wiese, N.R. Gliksman, C.E. Walczak, and Y. Zheng. 2001. Ran stimulates spindle assembly by altering microtubule dynamics and the balance of motor activities. *Nat. Cell Biol.* 3:221–227.